EnColor: Improving Visual Accessibility with a Deep Encoder-Decoder Image Corrector for Color Vision Deficient Individuals

Satyam Goyal[1], Kavya Sasikumar[2], Rohan Sheth[2], Akash Seelam[2], Taeyeong Choi[3], and Xin Liu[2]

[1] Electrical Engineering and Computer Science Department, University of Michigan, Ann Arbor, MI, USA
[2]Department of Computer Science, University of California, Davis, CA, USA
[3]Department of Information Technology, Kennesaw State University, Marietta, GA, USA
sagoyal@umich.edu, {ksasikumar, rsheth, aseelam, xinliu}@ucdavis.edu, tchoi3@kennesaw.edu

Abstract

Individuals with color vision deficiencies (CVDs) often face significant challenges in accessing vital information for decision-making. In response, we introduce EnColor—a deep **En**coder-decoder **Color** corrector for images, enabling individuals with CVDs to perceive the contents in originally intended colorization. Our network architecture is designed to effectively capture essential visual features for reconstructing standard images into color-corrected versions. In particular, our training pipeline is integrated with a CVD simulator so as to ensure the fidelity of output throughout the lens of individuals with impaired color vision. For evaluation, we focus primarily on tomato images, considering the profound impact of color vision deficiencies on practical domains like agri-food systems. Our quantitative results demonstrate that the EnColor model achieves over 16.8% improvement over previously introduced algorithms in terms of color retention, supporting our design choices. Furthermore, a survey with 43 participants provides subjective assessments with the highest scores on our method. Additionally, specific visual examples are presented to highlight accurately restored colors. We also publicly share all our codes of EnColor as well as the baseline methods to ensure reproducibility and facilitate more studies in CVD correction.

Introduction

Color plays a pivotal role in effective communication for decision-making. For instance, traffic lights use color to communicate road directions, leading to restrictions for those with color vision deficiencies (CVDs) (Parry 2015). Another example is illustrated, in Fig. 1, in which fruits become difficult to distinguish by color for people with CVDs. In real life, many individuals with CVDs struggle to identify ripe fruits (Cole 2004), raising a potential issue for farmers.

To address this problem, previous studies have introduced technological tools for adjusting original images to enhance *contrast*, so that individuals with CVDs could successfully identify distinct objects. (Lillo et al. 2022). These methods, however, employed simplistic, linear models with predefined parameters, and their main focus was on contrast enhancement rather than correcting images so that individuals with CVDs could see the image closer to what someone with normal color vision would see.

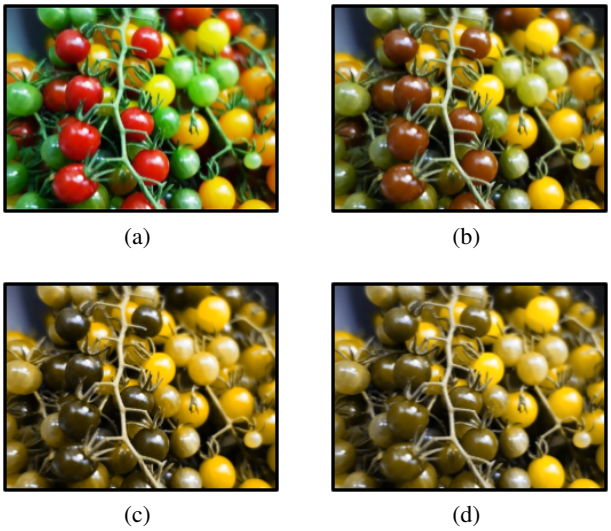

Figure 1: Simulations of different types of CVDs. (a) original, (b) dueteranomaly, (c) dueteranopia, and (d) protonopia

In this paper, we propose EnColor—a novel framework for an **En**coder-decoder **Color** corrector designed to learn the conversion of images into ones that *preserve* the original colors for viewers with CVDs. To be specific, as illustrated in Fig. 3, a deep convolutional encoder-decoder architecture is employed to automatically learn useful spatial features for color correction. In particular, EnColor involves a "CVD simulator" in the pipeline to calculate the loss function, specifically designed to assess image quality for individuals with CVDs. Additionally, we conduct experiments with tomato image data, taking into account the significant impacts of CVD on agricultural systems. Our quantitative evaluations show that the EnColor model can improve color restoration by over 16.8% compared to baseline methods. Furthermore, a survey with 43 participants provides subjective assessments with the highest scores on our method. Additionally, specific visual examples are presented to highlight accurately restored colors. We also release all our codes of EnColor and the baselines to promote reproducibility and further relevant studies[1].

[1]https://github.com/Satgoy152/EnColorExperiments

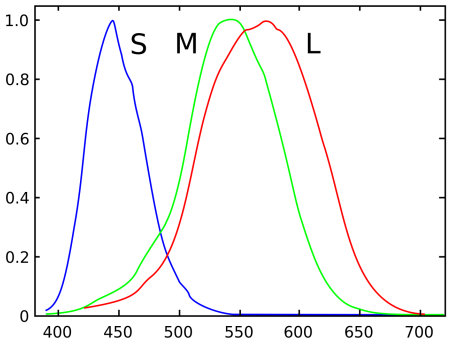

Figure 2: Spectral sensitivities of human cone cells: S, M, and L types. Curves are results of normalization with responsivity. (Plot by Vanessaezekowitz (2007))

The remainder of this paper is organized as follows. We first describe background knowledge of CVD to provide understanding of the phenomenon. Then, the next section explores previous relevant works on CVD simulations and automated color corrections. In the following section, we introduce our EnColor method with technical details. The descriptions of our experimental settings and results are then presented with discussion. Lastly, we conclude the paper with the summary of our work and future research plans.

Background: Color Vision Deficiency

In humans, color vision is facilitated by photosensitive cells, called cones, in the retina. Those cone cells can be categorized into three types based on their sensitivity to different wavelengths of light: long (L), medium (M) and short (S) (Hunt and Carvalho 2016), as visualized in Fig. 2.

CVDs occur when one or more of these cone categories are either missing (dichromacy or monochromacy) or altered (anomalous trichromacy) (Parry 2015). For example, the absence of L cones leads to *protanopia* (Fig. 1d), resulting in reduced sensitivity to red light. Similarly, individuals with no or defective M cones experience *deuteranopia* (Fig. 1c) or *deuteranomaly* (Fig. 1b), causing impaired perception of green wavelengths (Parry 2015).

Our EnColor model is designed to learn the synthesis of non-perceivable colors (e.g., red or green) using others, enabling individuals with CVDs to sense colors similar to the original (cf. Fig. 6). In particular, our experiments are conducted namely with simulations of deuteranopia and deuteranomaly because a review of the literature around CVDs by Birch (2012) reports that these red-green CVDs are the most prevalent conditions in the population.

Related Work

While the efficacy of specialized physical filters for CVDs have been extensively studied (Werner, Marsh-Armstrong, and Knoblauch 2020; Tanuwidjaja et al. 2014), software and algorithmic approaches in this domain remain relatively unexplored. Still, there are software tools designed primarily for content creators and designers to simulate CVDs. For instance, Color Oracle[2] and Sim Daltonism[3] can apply the filters of a particular CVD to computer screens so that designers can ensure that their visuals are accurately perceived. Game developers can also utilize similar tools, such as ones integrated into the Unity game engine[4] to assess vision-related accessibility issues. However, our work is distinct because it aims to assist individuals with CVDs directly. We not only automate the identification of problematic colors but also recolor the contents to enhance perception.

With similar motivations, Color Contraster (CC) (Yun, Michelson, and Brand 2007) was designed as a model for image enhancement for CVD, simply increasing the redness and greenness on pixels. As a consequence, this heuristic approach adds more contrast to these targeted pixels. Dody et al. (2019) also proposed a similar approach yet identified clusters of problematic colors in images. Their correction application is then targeted to the relevant clusters only.

Linear transformation models from (Petrovic and Fujita 2017) also enhance the contrast. More specifically, the original image and the image of the CVD simulation are compared to compensate for the difference by a multiplication a pre-defined matrix. Also, authors in (Lee and Santos 2010) introduced a "fuzzy logic-based" CVD correction algorithm. This method takes a weighted summation of two images generated for protanopia and deuteranopia, while the weights are dermined by fuzzy logic.

These models were namely designed to perform relatively simple, linear transformations with manually predefined parameters. In contrast, EnColor in our method can automatically use data to learn the parameters for conversion with non-linearity within neural networks. Furthermore, our experiments incorporate multiple evaluation metrics not only to quantify improved contrasts but also color restoration.

DeepCorrect (Petrovic and Fujita 2017) presents the most similar approach to ours since their framework also includes a deep neural network-based color corrector, involving a CVD simulator in the training loop. However, DeepCorrect leverages an adversarial learning setting in which a color corrector is trained to enhance RGB images while a referee network performs typical image-classification tasks on the enhanced images with CVD simulation applied. During training, the authors claim that the color-correction network learns to generate the images that are realistic even in the color space of CVD.

Yet, we claim that the abstract error signals for holistic image classification may not provide sufficient information to learn to synthesize similar colors to the original at each pixel location. Their outputs demonstrate this limitation because regenerated colors tend to appear dissimilar from the original ones. To tackle this issue, our EnColor instead directly compares the original RGB images with the simulated ones after color correction. This approach is to ensure the intended colors are successfully synthesized with other colors in receptive wavelengths. Additionally, we perform surveys with human participants.

[2]https://colororacle.org/

[3]https://github.com/michelf/sim-daltonism/

[4]https://unity.com/

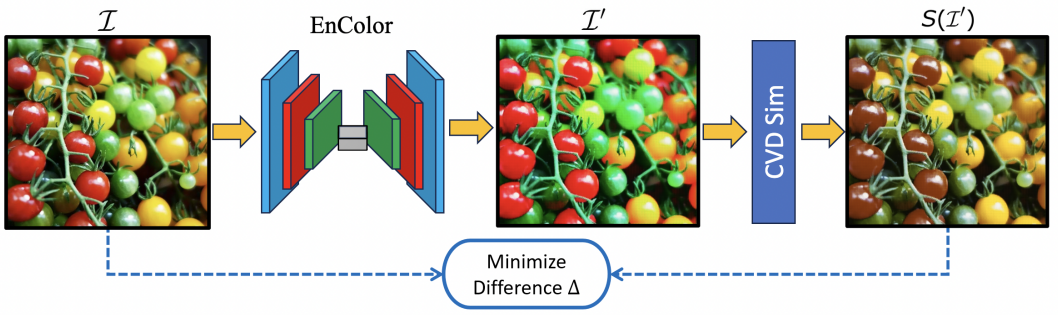

Figure 3: Illustration of the pipeline of color correction with EnColor, encoding and decoding an image $\mathcal{I}$ into a color-corrected image $\mathcal{I}'$. EnColor learns to generate $\mathcal{I}'$ minimizing the difference Δ between its CVD-simulated version $S(\mathcal{I}')$ and the original image $\mathcal{I}$.

(a) (b) (c) (d) (e)

Figure 4: Visualizations of varying degrees of deuteranomaly simulated: (a) Original, (b) 0.3, (c) 0.5, (d) 0.8, and (e) 1.0

Methodology

In this section, we describe two major components of EnColor with technical details: 1) a Neural network-based image corrector, and 2) a CVD simulator. In addition, our novel training process integrating both is introduced.

Image-Correction Network

Inspired by the successes of encoder-decoder architectures in image reconstruction (Badrinarayanan, Kendall, and Cipolla 2017; Mastan and Raman 2019), we incorporate them into the image corrector f of EnColor. To be specific, as illustrated in Fig. 3, the execution flow of the image corrector involves taking an ordinary RGB image $\mathcal{I}$ with dimensions $w \times h \times 3$ to encode it into an abstract representation and then decoding it into an altered image $\mathcal{I}'$ with the same dimensions as the input but modified colors.

Our image-correction network f employs convolutional layers to learn useful spatial patterns for color adjustment. More specifically, its encoder is built up with two convolutional layers with 16 and 8 3×3 kernels, respectively. In particular, each layer downsizes the input image by applying the kernels with a stride of 2, eventually producing a three-dimensional abstract representation v with dimensions $w' \times h' \times 8$. The decoder takes v as input to process it sequentially by two transposed convolutional layers with 16 and 8 3×3 kernels, respectively. Note that, as in the encoder, each decoding layer also uses a stride of 2 to enlarge images. Finally, an additional convolutional layer with three 3×3 kernels and a stride of 1 is applied to generate the output image $\mathcal{I}'$.

CVD Simulator

The CVD simulation function S is designed to return images with the colors that would be viewed by individuals with a particular type of CVD (cf. Fig. 4). Here, we leverage it to train our image corrector to generate images that are seen to be similar to the original by those with CVDs. (Machado, Oliveira, and Fernandes 2009)

Specifically, we employ a linear transformation to adjust the data within the red (R), green (G), and blue (B) channels, replicating the perceptual alterations occurring when "M" cones malfunction or are absent (Machado, Oliveira, and Fernandes 2009). Mathematically, we apply a 3×3 matrix to the RGB vector of each pixel in the image, thereby "shifting" the values to generate a simulated CVD image. Based on how much we shift the values in each channel, we can adjust the intensity α of CVD in simulation; for instance, deuteranomaly ($0 < \alpha < 1$) and deuteranopia ($\alpha = 1$). Figure 4 shows examples under various α values.

Specifically, the CVD simulator computes the following to convert a pixel with R, G, and B channels into simulated one, applying $\alpha = 0.5$ for simulation of deuteranomaly:

Intensity	0.1	0.2	0.3	0.4	0.5	0.6	0.7	0.8	0.9	1.0	Average
EnColor											
SSIM	0.934	0.929	0.932	0.918	0.923	0.922	0.916	0.915	**0.926**	**0.921**	0.923
MSE	137.68	144.97	**143.66**	**193.27**	**178.60**	**214.69**	**432.40**	**481.22**	640.75	798.89	**396.67**
Linear											
SSIM	**0.980**	**0.966**	**0.954**	**0.945**	**0.938**	**0.931**	**0.925**	**0.921**	0.918	0.915	**0.942**
MSE	**52.03**	155.36	273.37	390.32	500.19	600.91	691.72	773.53	847.34	913.68	559.82
CC											
SSIM	0.880	0.890	0.890	0.880	0.870	0.840	0.810	0.780	0.740	0.710	0.810
MSE	1028.71	800.74	624.86	518.92	510.19	641.34	969.85	1561.08	2463.14	3633.11	1225.22
Fuzzy											
SSIM	0.890	0.890	0.890	0.890	0.890	0.890	0.890	0.890	0.880	0.880	0.890
MSE	374.09	396.11	416.22	432.29	448.86	466.14	481.45	495.72	**507.78**	**518.74**	476.63
Cluster											
SSIM	0.960	0.940	0.920	0.890	0.870	0.840	0.810	0.780	0.750	0.730	0.850
MSE	59.16	**114.7**	196.9	304.16	437.13	594.36	776.33	981.20	1206.92	1452.48	612.33

Table 1: MSEs and SSIMs of tested methods under vaiours intensities of CVD. For each intensity, the best performance per metric is marked in bold. The right-most column provides the averaged performance over the intensities.

$$\begin{bmatrix} R_s \\ G_s \\ B_s \end{bmatrix} = \begin{bmatrix} 0.547494 & 0.607765 & -0.155259 \\ 0.181692 & 0.781742 & 0.036566 \\ -0.01041 & 0.027275 & 0.983136 \end{bmatrix} \begin{bmatrix} R_{in} \\ G_{in} \\ B_{in} \end{bmatrix}, \tag{1}$$

where R_{in}, G_{in}, and B_{in} represent values of input pixel in the R, G, B channels, respectively, while R_s, G_s, and B_s are the counterparts of simulated pixel. In particular, the constants in the transformation matrix were found experimentally by Machado, Oliveira, and Fernandes (2009) who developed a physiological-based model to estimate the interaction between cones in the eye. Also, for simulation of an entire image, the same conversion can be repeatedly performed across the pixels.

They provide different matrices tailored for various severity levels α to simulate. For instance, simulation of deuteranomaly ($\alpha = 1$) can be performed, using:

$$\begin{bmatrix} R_s \\ G_s \\ B_s \end{bmatrix} = \begin{bmatrix} 0.367322 & 0.860646 & -0.227968 \\ 0.280085 & 0.672501 & 0.047413 \\ -0.01182 & 0.04294 & 0.968881 \end{bmatrix} \begin{bmatrix} R_{in} \\ G_{in} \\ B_{in} \end{bmatrix}, \tag{2}$$

where compared to Eq. 1, each simulated channel C_s preserves the value from the original C_{in} to a lesser extent. Leveraging this flexibility in simulation, we conduct experiments under various conditions of CVD intensity.

Training Procedure

By leveraging the CVD simulator S, image corrector f is trained to optimize the simulated version of its output images I' to be similar to the original image $\mathcal{I}$ (cf. Fig. 3). More formally, our loss function computes the pixel-wise difference using mean absolute error between the images as below:

$$L(\theta) = \frac{1}{3n} \sum_{k=1}^{3n} |s_k - i_k|, \tag{3}$$

where $s_k \in S(f_\theta(\mathcal{I}))$, $i_k \in \mathcal{I}$, and $n = w \times h$—i.e., the total number of pixels.

This loss function guides the neural network to generate color-corrected pixels to be similar to the original $\mathcal{I}$ when a CVD has been applied. In other words, it can be minimized only when the generated images under CVD simulation exhibit the identical colors to the original. This aligns with our objective of enabling individuals with CVD to perceive the same colors from color corrected images $\mathcal{I}'$ as others would from the original $\mathcal{I}$.

Experiments

In this section, we show empirical results to demonstrate performance of EnColor. Firstly, the details of experimental settings are provided. Then, we present qualitative results in terms of two informative metrics, comparing to other baseline methods. Finally, qualitative analysis is offered based on collected answers from human subjects and notable example images.

Experimental Settings

Data & Baselines: For experiments, we mainly utilize the Laboro Tomato dataset[5], which comprises more than 600 high-quality images of real ripe and unripe tomatoes. This dataset presents a useful testbed to validate our method in practical environments such as agriculture.

For our testing, we reduced the image resolution to 648×484 to accelerate computation overall. Also, exclusive subsets of data were set up: training set of 600 images, validation set of 43, and test set of 150. For each experimental setup, EnColor was trained with the entire training set until the loss for the validation set started to increase. Moreover, the test set was used for performance reports of every method tested.

For comparative analysis, we adopt baseline image-correction methods mentioned above: *Linear* (Petrovic and

[5]https://github.com/laboroai/LaboroTomato

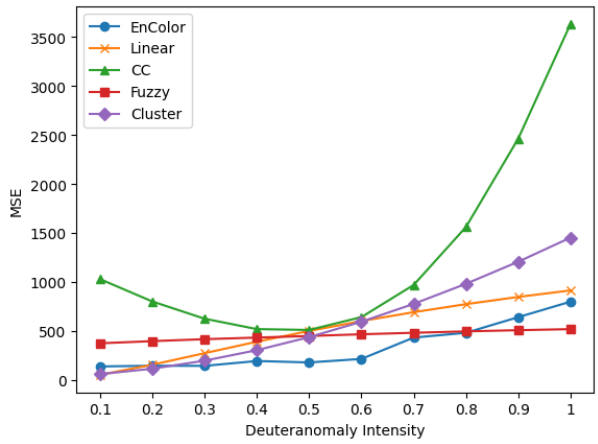

(a)

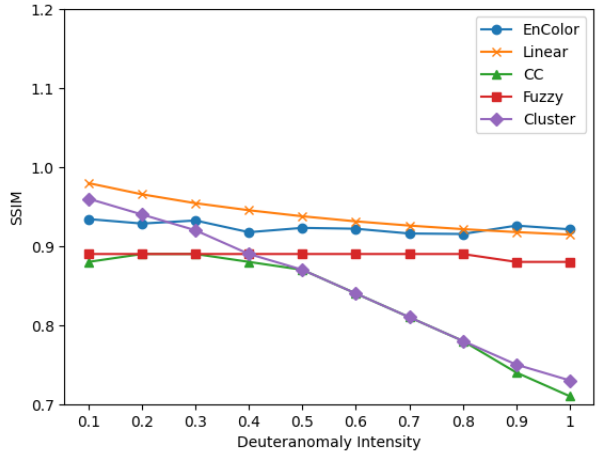

(b)

Figure 5: (a) MSEs and (b) SSIMs of tested methods for various intensities of CVD. For MSE, the lower the better, while for SSIM, the higher the better.

Fujita 2017), *Color Contraster (CC)* (Yun, Michelson, and Brand 2007), *Fuzzy* (Lee and dos Santos 2011), and *Clustering* (Dody et al. 2019). Because code for most the methods were not available, we implemented or reproduced them in Python, following the authors' instructions. We also release our codes to promote further relevant research using them.

Metrics: For evaluation, various severity levels of CVD are considered (i.e., 0.1 for weak deuteranomaly to 1.0 for deuteranopia). Specifically, two metrics are employed: Mean Squared Error (MSE) and Structural Similarity Index (SSIM) (Sara, Akter, and Uddin 2019). MSE is applied to quantify pixel-wise intensity differences between the input RGB image $\mathcal{I}$ and the simulated one $S(\mathcal{I}')$ after color correction applied. Note that we denote $S(\mathcal{I}')$ as $\mathcal{I}''$ hereafter unless mentioned otherwise.

For each input image $\mathcal{I}$, MSE is calculated as below:

$$\text{MSE} = \frac{1}{3n}\sum_{k=1}^{3n}(i''_k - i_k)^2, \tag{4}$$

where i''_k and i_k are kth pixel in $\mathcal{I}''$ and $\mathcal{I}$, respectively, and n is the total number of pixels.

In addition, SSIM is used to supplement our analysis, taking into account the luminance, contrast, and structure of compared images. More formally, we assess the quality of simulated output image $\mathcal{I}''$ by comparison with the original RGB image $\mathcal{I}$ as follows:

$$\text{SSIM}(\mathcal{I}, \mathcal{I}'') = \frac{(2\mu_{\mathcal{I}}\mu_{\mathcal{I}''} + C_1)(2\sigma_{\mathcal{I}\mathcal{I}''} + C_2)}{(\mu^2_{\mathcal{I}} + \mu^2_{\mathcal{I}''} + C_1)(\sigma^2_{\mathcal{I}} + \sigma^2_{\mathcal{I}''} + C_2)}, \tag{5}$$

where $\mu_{\mathcal{I}}$ and $\mu_{\mathcal{I}''}$ are the local means of images $\mathcal{I}$ and $\mathcal{I}''$; $\sigma_{\mathcal{I}\mathcal{I}''}$ is the covariance; $\sigma^2_{\mathcal{I}}$ and $\sigma^2_{\mathcal{I}''}$ are the local variances; and C_1 and C_2 are some constants used for stability in the division (Bae and Kim 2015). In particular, local statistics are obtained within a spatial window of size 11 to examine quality in local areas. Then, the multiple local SSIM's are averaged to obtain the final, global index for the input image pair. In particular, local statistics are obtained within a spatial window of size 11 to examine quality in local areas. Then, the multiple local SSIM's are averaged to obtain the final, global index for the input image pair.

While MSE always returns a value greater than or equal to 0, the output of SSIM is bounded between -1 and 1. Furthermore, larger MSEs mean more dissimilar images, whereas the maximum SSIM indicates that the images are the same. Also, a smaller SSIM indicates more of a difference between the two images.

Quantitative Results

Figure 5a visualizes variations in color retention while the severity of CVD changes. While CC presents declining errors from 0.1 up to 0.5 and an exponential increase with $>$ 0.5, other methods tend to consistently struggle with higher degrees of CVD. This is expected particularly in the case of EnColor, it has to generate output $\mathcal{I}'$ that appears more distinct from input $\mathcal{I}$ to compensate for more severe manipulation through the CVD simulation. Moreover, our EnColor was not the best model for low CVD levels ($0.1 \sim 0.2$), but its MSE increased at a *slow* phase between the CVD level of 0.3 and 0.8, which is the most common range in real world (deuteranomaly) (Tanuwidjaja et al. 2014). While at the worst CVDs ($0.9 \sim 1.0$), Fuzzy outperformed the model proposed in this paper, it still exhibited the second lowest errors.

Table 1 indicates that in average, Encolor provides 16.8% and 29.1% better performance than Fuzzy and Linear, respectively. This implies that the corrected images by EnColor can more likely visualize the originally intended colors for individuals with CVDs. In other words, EnColor successfully learns the synthesis of problematic colors using others in the CVD color space.

In terms of SSIM, Fig. 5b plots the evaluation results. As in the case of MSE, every method tends to lead to worse performance as the severity of red-green color blindness

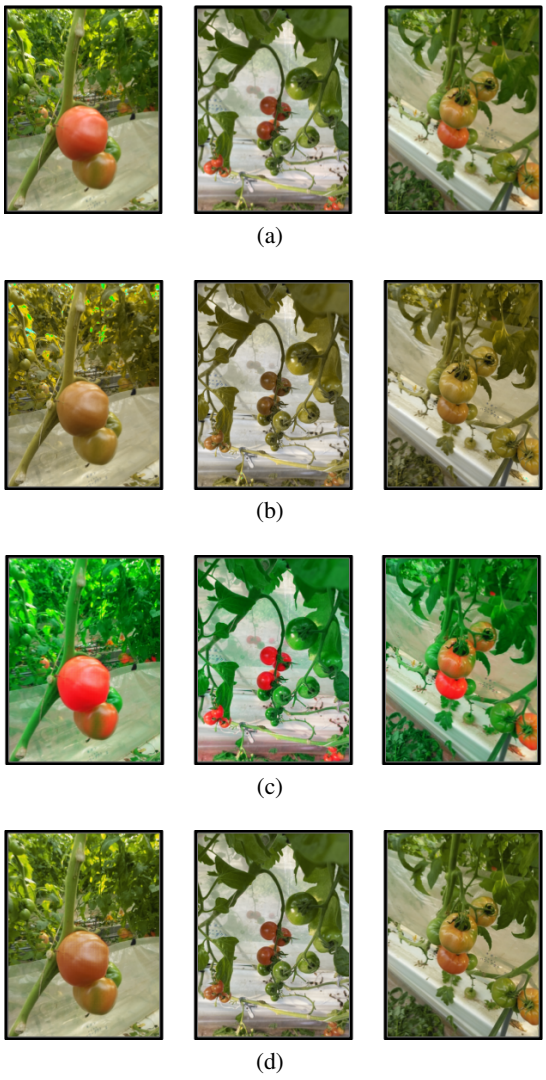

Figure 6: (a) Original images; (b) Original simulated; (c) Corrected; and (d) Corrected Simulated. Corrections were applied by EnColor under $\alpha = 0.5$ for simulations.

climbs. Also, from the degree of 0.5 onward, the performance of both Color Contraster and Clustering continue to drop, which is consistent with the MSE evaluation. EnColor, however, exhibits relatively reliable performance at various intensity levels, even though the Linear model marginally outperforms it by 2.1% for the levels up to 0.8. Nonetheless, EnColor achieves the lowest rate of decrease, showing 0.8% better performance than Linear at the extreme cases at the levels of 0.9 and 1.0 (cf. Table 1).

Overall, EnColor is the only method, which produces high-quality color correction for both MSE and SSIM.

Qualitative Analysis

Survey: To achieve a more comprehensive understanding of the effectiveness of color correction models, we also conducted a survey, soliciting the opinions of human participants with CVDs. We recruited 43 participants from social media (Instagram, Whatsapp, LinkedIn, etc.) for around 10 days. Among 43 individuals, 39 self-reported no CVD, while 4 reported a CVD. On the Qualtrics online platform[6], we first verified their CVD with questions from the Ishihara plates (Petrovic and Fujita 2017). If they had CVD, we displayed three unique tomato images (Fig. 6) that were color-corrected by all correction methods. Otherwise, simulated versions of the same images are shown to mimic how individuals with CVD would view them. For each image, participants were asked to subjectively evaluate contrast, ease of identifying ripe tomatoes, color retention, and overall preference.

	Linear	**Cluster**	**EnColor**	**CC**	**Fuzzy**
Contrast	3.19	2.11	**1.59**	2.46	3.99
Ripeness	2.98	1.79	**1.45**	2.14	3.47
Retention	25.98	**39.63**	33.08	3.37	0

Table 2: Participants ranked contrast and ease of identifying ripe tomatoes on a scale of 1-5, with lower scores indicating superior performance. Rows 1 and 2 display the average scores, while Row 3 presents the percentage of respondents who believe a method has superior color retention, with bold indicating the best performance for all.

In particular, Table 2 shows that participants provided the best average scores for the images corrected with EnColor for both contrast and ripeness-related evaluations, which are key factors that impact effectiveness for color-correction models; they had scores of 1.59 and 1.45 respectively on a scale from 1-5 (with 1 being the best). This human preference further supports our model as a useful tool for improving information delivery for those with CVDs. Overall, the balanced performance of EnColor, proven by the quantitative evaluations, is a key factor in producing images that are effectively received by humans.

In spite of these insightful findings, there are limitations that need to be considered in this survey. For instance, the sample size of the group with CVDs was small. Though we incorporated data from the non-CVD group, it remains unknown whether their perception of simulated images can perfectly emulate that of corrected images viewed by those with CVDs.

Examples: Figure 7 displays simulation examples of color-corrected images by all tested methods. The output of EnColor (Fig. 7c) appears most similar to the original (Fig. 7a), while that of Cluster (Fig. 7f) may be considered to be the second best. This observation is consistent with the finding from the survey.

Conclusion & Future Work

Color vision deficiency (CVD) presents a significant challenge that demands an effective solution, particularly given

[6]https://www.qualtrics.com/

Figure 7: Simulated results for all baselines and EnColor under intensity $\alpha = 0.5$: (a) Original, (b) *Linear*, (c) *EnColor*, (d) *Fuzzy*, (e) *CC*, and (f) *Cluster*

its implications in contexts such as farming, where the ability to distinguish between ripe and unripe fruits/vegetables is crucial. In this paper, we have proposed EnColor—a novel framework for an Encoder-decoder Color corrector capable of learning the transformation of RGB images into ones that preserve originally intended colors for individuals with CVDs. Our training scheme with CVD simulators has yielded significant improvement compared to other baseline methods, leading to the highest color retention rates on average.

We have also conducted a qualitative analysis using a form of human survey. Its results indicate that 43 participants assessed EnColor's color correction as the best when asked about both the visual contrast and the ease of classifying ripe fruits from corrected images.

All these results highlight the potential of EnColor as a tool for enhancing *accessibility in visual communication*. We publicly share all the codes used for our experiments to encourage further research in this area. In particular, our designs of algorithms and experiments can serve as a useful guideline for future investigations.

Potential future work includes training more sophisticated neural network models across domains beyond agriculture. To further improve the quality of produced images, the learning paradigm of Generative Adversarial Networks (GANs) could be incorporated into the framework. Furthermore, a modification to the loss function of EnColor in Eq. 3 could be explored, possibly incorporating SSIM or a proxy form into training. Furthermore, we recognize the importance of developing methods to identify the personal intensity of CVDs, enabling adaptive utilization of specialized color alteration algorithms tailored to individual needs.

References

Badrinarayanan, V.; Kendall, A.; and Cipolla, R. 2017. Segnet: A deep convolutional encoder-decoder architecture for image segmentation. *IEEE transactions on pattern analysis and machine intelligence*, 39(12): 2481–2495.

Bae, S.-H.; and Kim, M. 2015. A novel SSIM index for image quality assessment using a new luminance adaptation effect model in pixel intensity domain. In *2015 Visual Communications and Image Processing (VCIP)*, 1–4.

Birch, J. 2012. Worldwide prevalence of red-green color deficiency. *J. Opt. Soc. Am. A*, 29(3): 313–320.

Cole, B. L. 2004. The handicap of abnormal colour vision. *Clinical and Experimental Optometry*, 87(4-5): 258–275.

Dody, Q. U.; Tati, L. R. M.; Richard, M.; Andika, P. G.; and Tauhid, N. A. 2019. RGB color cluster and graph coloring algorithm for partial color blind correction. In *MATEC Web of Conferences*, volume 255, 01002. EDP Sciences.

Hunt, D. M.; and Carvalho, L. S. 2016. *The Genetics of Color Vision and Congenital Color Deficiencies*, 1–32. Cham: Springer International Publishing. ISBN 978-3-319-44978-4.

Lee, J.; and dos Santos, W. P. 2011. An adaptive fuzzy-based system to simulate, quantify and compensate color blindness. *Integrated Computer-Aided Engineering*, 18(1): 29–40.

Lee, J.; and Santos, W. 2010. An adaptative fuzzy-based system to evaluate color blindness. In *Proceedings of the 17th International Conference on Systems, Signals and Image Processing (IWSSIP 2010), Brazil, Rio de Janeiro*.

Lillo, J.; Moreira, H.; Abad, L.; and Álvaro, L. 2022. Daltonization or colour enhancement: potential uses and limitations. *Optics Express*, 30(25): 45156–45177.

Machado, G. M.; Oliveira, M. M.; and Fernandes, L. A. 2009. A physiologically-based model for simulation of color vision deficiency. *IEEE transactions on visualization and computer graphics*, 15(6): 1291–1298.

Mastan, I. D.; and Raman, S. 2019. Multi-level encoder-decoder architectures for image restoration. In *2019 IEEE/CVF Conference on Computer Vision and Pattern Recognition Workshops (CVPRW)*, 1728–1737. IEEE.

Parry, N. R. 2015. *Color vision deficiencies*, 216–242. Cambridge Handbooks in Psychology. Cambridge University Press.

Petrovic, G.; and Fujita, H. 2017. Deep Correct: Deep Learning Color Correction for Color Blindness. In *SoMeT*, 824–834.

Sara, U.; Akter, M.; and Uddin, M. S. 2019. Image quality assessment through FSIM, SSIM, MSE and PSNR—a comparative study. *Journal of Computer and Communications*, 7(3): 8–18.

Tanuwidjaja, E.; Huynh, D.; Koa, K.; Nguyen, C.; Shao, C.; Torbett, P.; Emmenegger, C.; and Weibel, N. 2014. Chroma: a wearable augmented-reality solution for color blindness. In *Proceedings of the 2014 ACM international joint conference on pervasive and ubiquitous computing*, 799–810.

Vanessaezekowitz. 2007. Spectral sensitivities (normalized responsivity spectra) of human cone cells, S, M, and L types. https://en.wikipedia.org/wiki/Spectral_sensitivity#/media/File:Cones_SMJ2_E.svg. Accessed: 2023-07-30.

Werner, J. S.; Marsh-Armstrong, B.; and Knoblauch, K. 2020. Adaptive changes in color vision from long-term filter usage in anomalous but not normal trichromacy. *Current Biology*, 30(15): 3011–3015.

Yun, T.; Michelson, J.; and Brand, Z. 2007. COLOR CONTRASTER.